Express Polymer Letters Vol.17, No.5 (2023) 487–501
Available online at www.expresspolymlett.com
https://doi.org/10.3144/expresspolymlett.2023.36

Research article

A new composite nanofibrous biomaterial development for drug delivery applications

Hülya Kesici Güler[*], *Funda Cengiz Çallıoğlu*

Süleyman Demirel University, Engineering Faculty, Textile Engineering Department, 32260 Isparta, Turkey

Received 19 July 2022; accepted in revised form 9 December 2022

Abstract. This study aims to produce drug delivery systems using ultrasonic spray pyrolysis (USP) and electrospinning methods. For this purpose, the study was carried out in two steps. In the first step, polyvinylpyrrolidone (PVP)/gelatin (GEL) based nanofibers were produced by the electrospinning method. The nanofibers were coated with azithromycin (AZI) in the second step using the USP method. Finally, characterization studies such as morphological, chemical, and thermal were carried out, and drug release behaviors were analyzed. The findings show that nanofibers are noticeably fine, smooth, and uniform. Although burst release was observed for the first time because the drug molecules were located on the nanofibrous surface, the release time was increased from 30 min to 48 h by obtaining sandwich structures. The results showed that the USP method could be used to produce new drug delivery systems with the electrospinning method.

Keywords: *biopolymers and biocomposites, electrospinning, nanocomposites, nanomaterials, polymeric drug delivery systems*

1. Introduction

Pharmaceutical nanotechnology has gained the interest of many researchers in recent years due to its multiple benefits. The use of nanostructures in drug delivery systems has been researched for its potential to lead to the development of novel dosage forms that have increased therapeutic potential while reducing toxicities [1]. Poorly water-soluble drugs may cause challenges in terms of lower drug potency and effectiveness. The bioavailability of drugs is highly dependent on their solubility in water. As is known from the literature, for the most part, the bioavailability of drugs that dissolve in small amounts of water is low. To date, one of the most challenging issues in drug research has been the effort to increase the dissolution and solubility of a poorly water-soluble drug [2]. Many methods are utilized to enhance drug dissolving rates, including electrospinning [3], solid dispersion [4], chemical modification [5], cosolvency [6], and pH adjustment [7]. Drug-loaded electrospun nanofibers are frequently used for pharmaceutical applications, such as spironolactone-loaded nanofibers [8], triclosan-loaded polycaprolactone nanofibers [9], tetracycline-loaded polycaprolactone nanofibers [10], donepezil loaded poly (vinyl alcohol) (PVA) nanofibers [11]. Moreover, the solubility of drugs in nanofibrous structures and casting film structures were compared. For this, ketoprofen-loaded PVA nanofibers and PVA casting films were used. They determined that the electrospinning method is a method that can be used to improve the dissolution of the drug due to the high specific surface area and the conversion of the crystalline structure of the drug into amorphous. In another study, the electrospinning of thiram/hydroxypropyl-β-cyclodextrin inclusion complex nanofiber (thiram/HPβCD-ICNF) was produced for establishing quick-dissolving water-based drug delivery system. Thiram is a water-insoluble broad-spectrum fungicide, and the solubility of this drug has been investigated. It has

[*]Corresponding author, e-mail: hulyakesici@sdu.edu.tr

been determined that the drug trapped in the structure of nanofibers has better solubility, better antifungal activity, and better thermal stability than that of the pure drug [12].

Polyvinylpyrrolidone (PVP) is a biocompatible, non-toxic, water-soluble, hydrophilic, and synthetic polymer whose use in nanofibrous surfaces for biomedical purposes has been investigated in the literature [13–17]. Irbesartan-loaded PVP nanofibers with low bioavailability, known as a drug with poor water solubility, were produced, and dissolution studies were carried out. Irbesartan-loaded PVP nanofibers with low bioavailability, known as a poor water solubility drug, were produced, and dissolution studies were carried out. It was determined that drug-loaded nanofibers tested in different characterization analyses and *in vivo* showed increased bioavailability compared to Irbesartan plain suspension [18].

Azithromycin (AZI) is a macrolide antibiotic with low water solubility, with 15 members developed from erythromycin. The antibacterial activity and pharmacokinetic properties of AZI have been found to be superior to those of erythromycin. Due to the compound's broad antibacterial activity and low toxicity, it is an excellent candidate for particle size reduction with the objective of enhancing antimicrobial activity while decreasing toxicity [1]. In the kinetic studies performed with AZI, it was determined that AZI showed first-order reaction kinetics. Zhang *et al*. [19] investigated the kinetics of AZI degradation. For this, degradation kinetics were investigated as functions of pH (4.0–7.2), buffer composition (phosphate, acetate, and citrate), buffer concentration, ionic strength, drug concentration, and temperature. According to the results, the rate of degradation of AZI was found to be independent of its initial concentration, with maximum stability occurring at about pH 6.3 at 0.05 mol/dm^3 potassium phosphate. Moreover, it was observed that the observed degradation rate and ionic strength increased with buffer concentration [19]. There are limited studies in the literature on AZI-loaded nanofibers. [20] suggest that AZI-loaded chitosan/polyvinylalcohol/polyvinyl pyrrolidone (CS/PVA-PVP) with long-term antibacterial activity by electrospinning method faces some challenges that can be overcome by the application of new drug delivery systems, such as conventional topical dosage forms, low intraocular bioavailability. According to the results, all formulations were determined to be uniform, fine, and smooth the nanofibers had a diameter range of 119–171 nm. It has been determined that the nanofiber is non-irritating and non-toxic to the eyes of rabbits. In the release test results, it was concluded that crosslinked AZI nanofibers showed slower and more controlled drug release in tear fluid compared to uncrosslinked ones for 184 hours (6–8) days. [21] aimed to produce a nanofiber drug delivery system capable of sustained release with minimized burst release from AZI-loaded PCL nanofibers to develop and characterize polycaprolactone (PCL) and chitosan (CS) based electrospun composite nanofiber membranes. A 25 day *in vitro* drug release analysis revealed that drug release from composite electrospun PCL/CS membranes is controlled by different mechanisms at different time periods. During the first few days, the drug release was controlled by the desorption mechanism of drug molecules on the surface of the nanofibers, as well as the diffusion of some drug molecules near the surfaces of the nanofibers, after this stage, the swelling of the CS nanofibers reduced the pore size of the membrane, resulting in slower drug diffusion and more appeared with a decreasing rate of release afterwards. Over time, drug release was mainly affected by the degradation of the CS fibers, resulting in the transport of remaining drugs through the pores formed within the degraded CS nanofibers.

Ultrasonic spray pyrolysis (USP) has long been utilized in industry for the continuous fabrication of ultrafine powders and nanoparticles [22]. The USP method is a low-cost, feasible, simple, convenient, facile, and applicable method [23, 24]. The USP method, which has been utilized and developed for years in a variety of application areas, is used to create magnetic, optical, semiconductor, and superconducting thin films and particles. There are numerous advantages of this method, including the ability to produce spherical and non-agglomerated particles with a wide range of chemical composition, size, and morphology. The USP method is widely used, especially in the production of nanospheres such as $CaMoO_4$: Eu^{3+} [13], $MgFe_2O_4$ [14], and $NiCo_2O_4$ [15]. At the end of the treatment, submicron-sized uniform spherical particles are produced [23]. New materials produced by this method have been used as catalysts [17], sensors [16], electronic [25] and magnetic [26] materials, and more. In the literature, there are limited studies related to USP and drug delivery systems, such as nanospheres [27] and microspheres [28, 29]. Despite this, there is no evidence that a drug

delivery system can be made using the USP method with nanofibers.

The aim of this study is to introduce a new drug delivery system preparation technique that can produce both immediate and slow releases in the literature.

2. Experimental

2.1. Materials

PVP ($M_w = 0.36 \cdot 10^{-6}$ g/mol) was used as a polymer, gelatin (GEL) from porcine skin (gel strength 300, Type A) was used as a co-polymer, ultra-pure water (UPW) and acetic acid (AA) (Reagent Plus, ≥99%) were used as solvents for polymers, azithromycin (AZI) (M_w = 785.02 g/mol) was used as a model drug. Chloroform (containing 100–200 ppm amylenes as a stabilizer, ≥99.5%) and *n*-hexane (VWR Chemicals, assay 98%) were used as solvents for preparing AZI solution. Glutaraldehyde solution (GTA) (Grade II, 25% in H_2O) was used as a crosslinker, phosphate buffered saline (PBS) (pH 7.4), ethanol (absolute ≥99.8%) and NaOH (M_w 40.00, 98–100.5%, pellets) were used for drug release medium. PVP, GEL, AA, chloroform, AZI, GTA, PBS, ethanol, and NaOH were purchased from Sigma-Aldrich Corporation (St. Louis, MO, USA), and ultra-pure water was obtained from a Millipore Milli-Q System with a conductivity of 18.0 MΩ·cm.

2.2. Methods

This study was carried out in two steps. In the first step, nanofiber mat production was carried out by electrospinning. For this, PVP concentration was kept constant as 12 wt% and GEL concentration as 0.72 wt% from our previous optimization studies. Then, solution properties such as viscosity (Lamy Rheology, B-One Touch Screen, France) under a shear rate of 5 s^{-1}, conductivity (SelectaCD2005, Spain), surface tension with Du Noüy Ring method (Biolin Scientific Sigma 702, Finland) and pH (Adwa 1110, Hungary) were measured. All measurements were carried out at room temperature. Finally, the production of PVP/GEL nanofibers at optimum process parameters was carried out by an atmosphere-controlled horizontal needle laboratory scale electrospinning method. During fiber spinning, all solutions were produced in equal time with the same process parameters. The produced nanofibers were collected on aluminum foil. The optimum process parameters applied during fiber spinning are given in Table 1.

In the second step of the study, it is the thin film coating of AZI on PVP/GEL nanofibrous surfaces with the ultrasonic spray pyrolysis (USP) (Sono-Tek, FlexiCoat, USA) method. The first and most basic stage of the system is aerosol formation. Here, aerosol formation takes place with a high frequency of up to 100 MHz. Then, the formed droplets are transported to the furnace with a temperature above 200 °C by means of carrier gas. Nitrogen is used as the carrier gas. Evaporation/drying, precipitation, and fragmentation occur in droplets in contact with high temperatures. Diffusion occurring at this stage causes particle formation by thermal degradation or reduction. Parameters affecting the particle size, size distribution, and morphology of the final product during the whole process; properties and concentration of the starting solution, the amount of temperature, the effect of the flow rate of the carrier gas, and the effect of the operating frequency [30]. To be used in the USP method, the AZI was dissolved in chloroform, and the AZI concentration was adjusted to be 0.3 mg/ml. To prevent chloroform from dissolving and damaging the nanofiber surface, *n*-hexane was used as an antisolvent during the process. The process parameters applied for the USP method are given in Table 2.

Finally, thin film coating of PVP/GEL (USP0) nanofibers with various AZI concentrations of 0.1, 0.3, 0.5, 0.7, and 0.9 wt% has been performed. Nanofibers were produced from a PVP/GEL polymer solution

Table 1. Process parameters of the electrospinning method.

Voltage [kV]	Distance between electrodes [cm]	Feed rate [ml/h]	Humidity [%]	Temperature [°C]	Needle inner diameter [mm]	Production time [min]
26.4	17.0	0.3	33±2	23.5±1	0.8	60

Table 2. Process parameters of the USP method.

Flow rate [ml/min]	Substrate temperature [°C]	Distance between nozzle and substrate [cm]	Nozzle frequency [kHz]	Forming (nitrogen) gas pressure [kPa]
1	100	13	85	1

for 1 hour. The resulting nanofibers were weighed (40 mg). Before coating the nanofibers with AZI using the USP method, 5 different nanofibers for 1 hour were produced for 5 different concentrations. The weight of all of them is accepted as theoretically being the same. The amount of AZI to be coated was calculated in mg by proportioning the weight of the polymers in the polymer solution to the weight of the AZI to be coated. Finally, the volume of the coating solution was calculated based on the AZI concentration in the AZI/chloroform/hexane solution. In Table 3, the codes of the samples produced for this method and the amounts of coating AZI/chloroform/*n*-hexane solution used are given.

Images were taken with FEI Quanta 250 FEG scanning electron microscope (SEM) at ×5000 and ×20 000 magnifications in order to analyze the morphology of nanofibers. From SEM images, the diameter of 100 different fibers was measured for each sample from different part of the nanowebs with the ImageJ image analysis software. Then, the fiber diameter uniformity coefficient was calculated by calculating the number and weight averages according to the Equations (1) and (2) [31]:

$$A_n = \frac{\sum n_i d_i}{\sum n_i} \text{ (average number)} \quad (1)$$

$$A_w = \frac{\sum n_i d_i^2}{\sum n_i d_i} \text{ (average weight)} \quad (2)$$

where d_i: fiber diameter, n_i: number of fibers.

In the same way as the molar mass distribution principle, the A_w/A_n ratio gives the fiber diameter uniformity coefficient. In this equation, the closer the result is to 1, the more uniform the fibers are [31].

The presence of model drug and polymers in the structure of nanofibers was determined chemically with a Perkin Elmer Spectrum BX and a 2 cm^{-1} resolution between 400–4000 cm^{-1} wavenumbers using KBr disc technique by Fourier transform infrared spectroscopy (FT-IR) analysis.

Table 3. Sample codes and solution amounts used in the USP method.

Samples codes	AZI concentration [%]	Amount of AZI solution used for coating [µl]
USP0.1	0.1	942
USP0.3	0.3	2826
USP0.5	0.5	4716
USP0.7	0.7	6600
USP0.9	0.9	8460

Thermogravimetric analysis (TGA) was carried out with an Exstar SII TG DTA 7200 to examine the thermal stability of nanofibers, polymers, and the model drug in a nitrogen gas environment by increasing 10 °C/min from room temperature to 600 °C with an approximately 5.5 mg sample.

Differential scanning calorimetry (DSC) analysis was carried out with Perkin Elmer DSC 4000 to determine the glass transition, melting, and decomposition temperatures and enthalpies of nanofibers, polymers, and the model drug in a nitrogen gas environment from 24 to 600 °C, increasing by 10 °C/min with an approximately 4.5 mg sample.

X-ray diffraction (XRD) analyzes the crystallinity of nanofibers, polymers, and drug substances that were analyzed with the Bragg-Brentano method at a wavelength of 1.54060 Å using a Bruker brand D8 Twin with Cu K_α irradiation between 2θ: 5–60°.

The calibration curve was calculated with the Peak Instruments T-9200 dual-beam ultraviolet and visible light absorption spectrophotometer (UV-vis) device of AZI, which is the model drug.

Since the model drug is lipophilic and does not dissolve in pH 7.4 phosphate-buffered saline (PBS), PBS:ethanol (9:1) was used as the dissolution medium, and the pH value of the dissolution medium was adjusted to 7.4 with 10% NaOH solution. Then, for plotting, 30 different solution between 2.5 and 75 µl were used with PBS:ethanol (9:1) solution. The absorbance values of these solutions were measured in a UV-vis device using PBS:ethanol (9:1) solution at a wavelength of λ_{max} = 202 nm as a blind [32]. Three measurements were made for each concentration value, and the average value was taken. By putting the obtained absorbance values against the concentration, the calibration curve was calculated, and the equation was obtained.

Before drug release experiments, crosslinking studies were carried out in order to prevent the dissolution of nanowebs in the dissolution medium and to increase their stability. Briefly, to crosslink PVP and GEL polymers, the nanowebs were first treated in a vacuum oven at 180 °C for 4 hours, then in GTA vapor at 24 °C for 24 hours [33]. Nanofibers were weighted average 40 mg and taken into the dissolution medium. Then, incubation was carried out at 37 °C and a shaking speed of 50 pm. A sample of

Table 4. Sample codes and contents of sandwich structures.

Sample codes	Bottom layer production time [min]	AZI concentration [%]	Upper layer production time [min]
USP0.7-5	60	0.7	5
USP0.7-15	60	0.7	15
USP0.7-30	60	0.7	30
USP0.7-45	60	0.7	45
USP0.7-60	60	0.7	60

1 ml of dissolution medium was taken at specific interval times. After the UV-Vis measurements at 202 nm wavelength, the 1 ml samples were replaced in the dissolution medium. The amount of AZI released was determined by putting the measured absorbance values on the calibration curve.

In the USP method, after the nanofiber surfaces were coated with different amounts of AZI solution given in Table 3, the release profiles were examined and the nanofiber surface containing 0.7% AZI (USP0.7); the most suitable one was chosen for the next step. Then, PVP/GEL nanofibers were produced for 1 h, and the surface of each was coated with 0.7% AZI. Sandwich structures were obtained by producing nanofibers for 5, 15, 30, 45, and 60 min on the surfaces coated with the USP technique (Table 4). The release profiles of these sandwich structures were also investigated.

3. Results and discussion

Firstly, the solution properties of PVP/GEL weremeasured. Results are given in Table 5.

Figure 1 shows SEM images of PVP/GEL nanofibers coated with AZI at different amounts with the USP technique.

When SEM images are analyzed, the increased coating time and amount are clearly visible on the surface of the nanowebs. As expected, the surface deformation increased with increasing coating time and amount. In general, nanofibers are fine and uniform in structure. Figure 2 shows the histogram of nanowebs with AZI coated with different concentration.

According to Figure 2, the diameters of PVP/GEL nanofibers coated with different concentrations of AZI were not affected by the USP coating as expected. The thicker fiber diameter in the USP0.7 and USP0.9 samples is thought to be due to optical illusion during fiber diameter measurement due to a large amount of coating solution. Apart from that, the fibers generally have a homogeneous fiber diameter distribution, and the fiber diameter distribution curve is unimodal. The average fiber diameter is 196.44 nm, and the standard deviation is 36.15 nm for USP0. While the thinnest fiber was 128 nm in nanoweb structure, the thickest fiber was measured at 324 nm. The fiber diameter uniformity coefficient is 1.0335.

In Figure 3, FT-IR spectra of PVP and GEL polymers, AZI, PVP/GEL (USP0) nanofibers, and AZI/PVP/GEL (USP0.7) coated nanofibers are given.

When the spectra were analyzed in detail, the O–H stretching peak of the hydroxyl group was seen at a wavenumber of 3434 cm^{-1} in the PVP spectrum. The alcohol O–H stretching vibration seen here at around 3600 cm^{-1} is the form of the water molecules absorbed on the PVP polymer, masked by a large O–H peak. The O–H peak appeared at 3446 cm^{-1} in USP0, at 3446 cm^{-1} in USP0.1, at 34476 cm^{-1} in USP0.3, at 3446 cm^{-1} in USP0.5, at 3447 cm^{-1} in USP0.7 and at 3445 cm^{-1} in USP0.9. The presence of heteromic molecules and carbonyl groups in the pyrrolidone ring of PVP was identified by the sharp peak at 1654 cm^{-1} as a sign of C=O stretching. Here, the vibrational frequency of the carbonyl stretch is very sensitive to hydrogen bond formation with water molecules. Therefore, as the concentration of absorbed water increases, this peak may shift from 1680 to 1652 cm^{-1}. The C–N stretch peak observed in the PVP spectrum at a wavelength of 1499 cm^{-1}, and it is appeared in the nanofiber samples is in USP0, USP0.1, USP0.3, USP0.5, USP0.7 and USP0.9 wavelengths of at 1494 cm^{-1}, at 1495 cm^{-1}, at 1494 cm^{-1}, at 1495 cm^{-1}, at 1495 cm^{-1}, and at 1495 cm^{-1}, respectively. In addition, the peak appearing at 1460 cm^{-1} wavelength in the PVP spectrum can be attributed to the C–H distortion deformation of the CH_2 group, and this peak was detected at 1460 and 1462 cm^{-1} wavelengths in all nanofiber samples. Moreover, CH_2 curling was detected at 1165 cm^{-1}, C–C ring was seen at 837 cm^{-1} in the fingerprint region, and N–C=O bending peak

Table 5. Polymer solution properties

Polymer solution code	pH	Conductivity*±STD** [µS/cm]	Viscosity±STD** [Pa·s]	Density [kg/l]	Surface tension±STD** [mN/m]
USP0	2.53	776±0.47	1.03±0.03	1.0306	54.01±0.48

*Conductivity value at 25±0.5 °C temperature

**STD: standard deviation

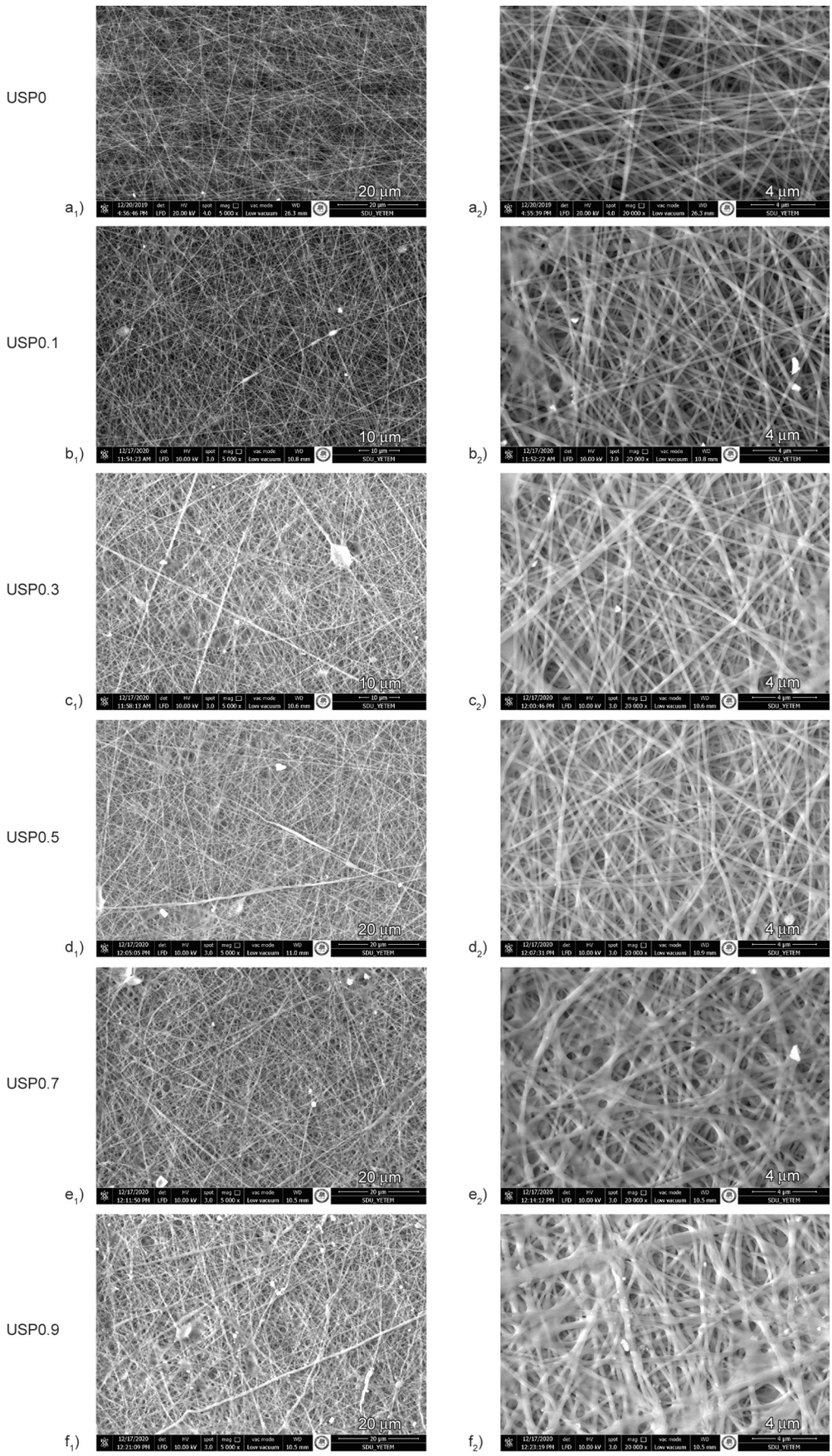

Figure 1. SEM images of different amounts of AZI-coated PVP/GEL nanofibers: a) USP0, b) USP0.1, c) USP0.3, d) USP0.5, e) USP0.7, f) USP0.9, a_1)–f_1) 5000× and a_2)–f_2) 20 000×.

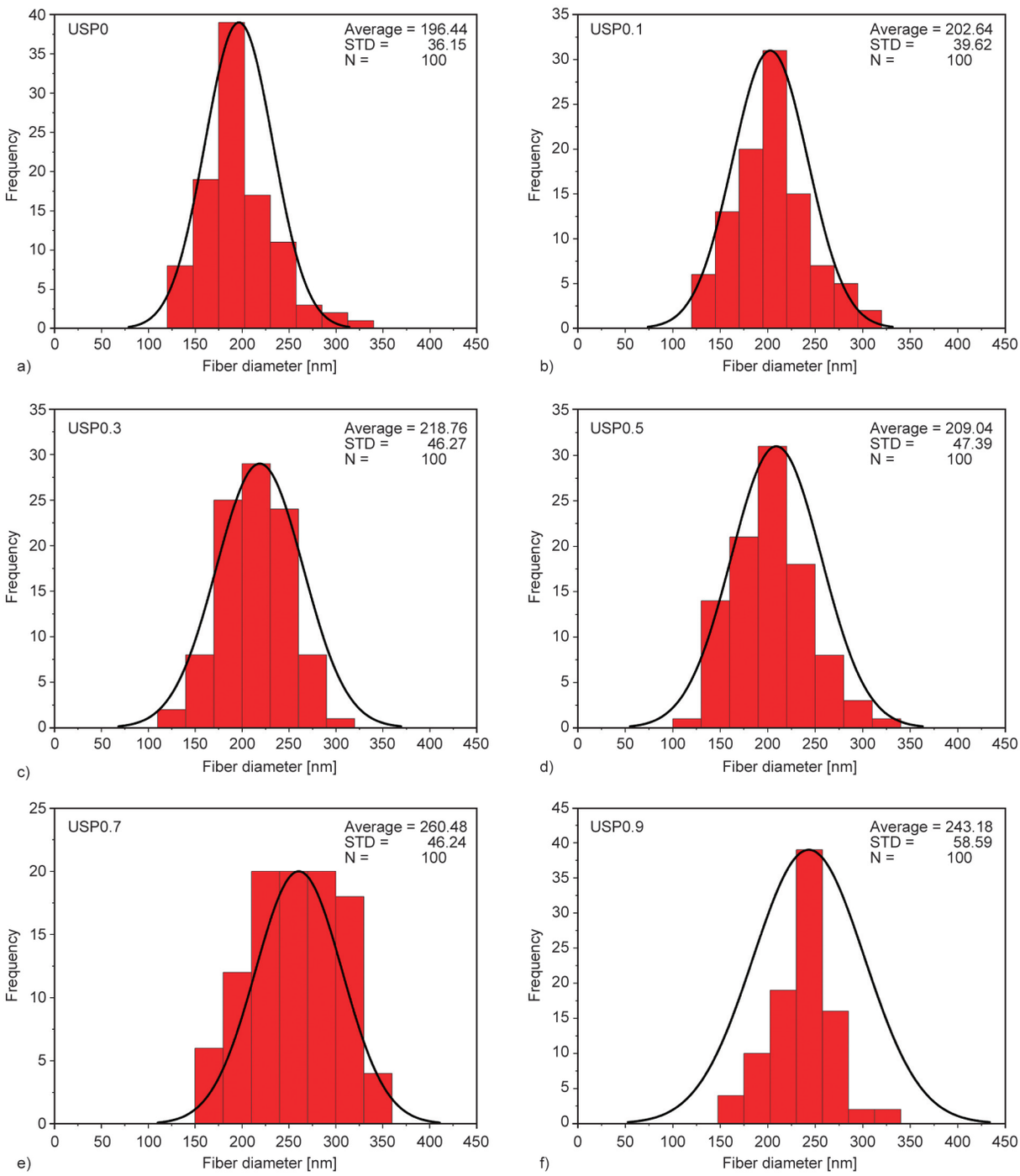

Figure 2. Histogram of nanowebs with AZI coated of different concentration. a) USP0, b) USP0.1, c) USP0.3, d) USP0.5, e) USP0.7, f) USP0.9. STD is the standard deviation, N is the number of measurements.

appearing at 583 cm^{-1} was also seen in the spectra of all nanofiber samples. To be evaluated in general, the presence of heteroatom and carbonyl group in the pyrrolidone ring reduces the symmetry sufficiently. Therefore, most of the vibrational modes exist at different intensities in the FT-IR spectra of both PVP and PVP-based nanofibers [34–39].

Characteristic amide-I (C=O stretching), amide-II (N–H bending and C–H stretching), and amide-III (C–N stretching) are seen prominently in the GEL spectrum at wavelengths of 1456, 1516, and 1232 cm^{-1}, respectively. The peaks are seen around these wavelengths in a way that has lost their intensity in the spectra of nanofibers. It is thought that the reason for losing their density is that they are used in low concentration during nanofiber production. In addition, a weak peak was observed in the GEL spectrum at a wavelength of 720 cm^{-1}. This can be

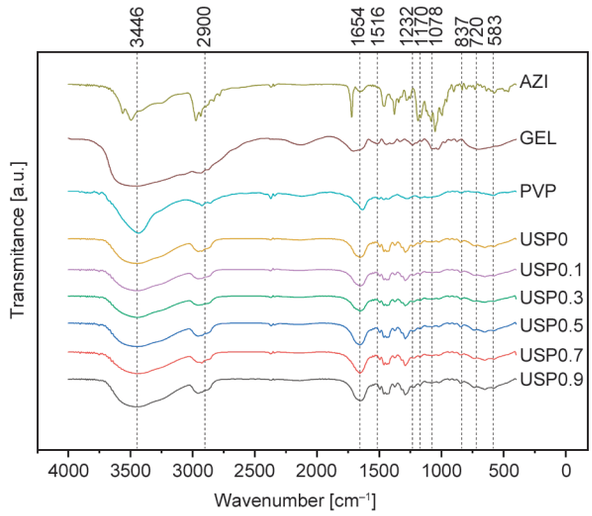

Figure 3. FT-IR spectra of PVP and GEL polymers, AZI, PVP/GEL, and AZI/PVP/GEL.

attributed to the $–CH_2–$ rocking vibration seen in samples with 4 or more consecutive CH_2 groups, as in the amino acid lysine, which is one of the important components of gelatin [40–44].

The OH stretching peak is seen at 3495, and 3562 cm^{-1} wavelengths in the AZI spectrum is due to tightly bound water molecules in the AZI crystal lattice. Other researchers stated that the double peak seen around the 3500 cm^{-1} wavelength decreased to a single broad peak in nanofiber spectra, which can be explained by the transition of AZI from crystalline form to amorphous form. Already in the DSC and XRD analyses carried out within the scope of the study, it has been determined that AZI transforms from crystalline form to amorphous form. Moreover, OH group peaks bending are also seen around 1458 cm^{-1} wavelength in the AZI spectrum. The C=O ether stretch peak seen in the AZI spectrum at a wavelength of 1188 cm^{-1} increased slightly from USP0.1 to USP0.9 in the nanofiber spectra, except for the USP0 sample and appeared at wavelengths of 1169, 1170, and 1171 cm^{-1}. The symmetrical aliphatic ether peak detected at 1051 cm^{-1} in the AZI spectrum decreased in general in the spectra of nanofibers, except for the USP0 sample but appeared as more prominent peaks with increasing AZI concentration. In addition, this peak was not near the wavelength of 1051 cm^{-1} in the spectrum of nanofibers but around the wavelength of 1078 cm^{-1}. This may be due to the Van der Waals forces formed between the AZI and the carrier, that is, the polymers. It has been determined from the FT-IR spectra that, in general, no undesirable chemical interaction between drugs and polymers is observed, and the basic characteristic peaks of AZI and polymers are clearly seen in the nanofiber spectra [1, 2, 45–47].

TGA thermograms of PVP/GEL nanofibers coated with AZI at different concentrations with the USP method are given in Figure 4.

When Figure 4 is examined in detail, it is clearly seen that AZI, PVP, and GEL show a one-step degradation. Due to the highly hydrophilic nature of PVP and GEL polymers, they lost 11.40 and 11.52% in weight, respectively, up to 100 °C due to the water molecules on them. The PVP polymer decomposed between 354.6 °C (t_0) and 478.1 °C (t_f) and left 5.72% residue at 600 °C. Similarly, the GEL polymer decomposed at a weight loss of 63.14% between 221.7 and 469.76 °C, and the sample had a mass of 25.34 wt% at the final temperature. While the GEL polymer rapidly realized 44.38% of the weight loss at 352.1 °C, it continued the remaining 18.76% slowly up to 600 °C. The 5.17% weight loss of AZI between 25–120 °C indicates the transition of AZI from the dihydrate to the anhydrous AZI form. This observed 5.17% weight loss corresponded to the stoichiometric weight loss of two water molecules [32, 48]. The decomposition temperature of AZI starts at 216.6 °C, similar to GEL polymer, and continues up to 472.3 °C. Meanwhile, it lost a mass of 91.46% and left a very low amount of residue, such as 3.37%, at the final temperature of 600 °C. Due to the water molecules in the nanofiber samples, weight loss was observed between 25 and 100 °C. In general, the temperatures at which nanofibers begin to degrade are between 306.9 and 354.1 °C. Similarly, the temperature at which the mass loss ends is very close to each other,

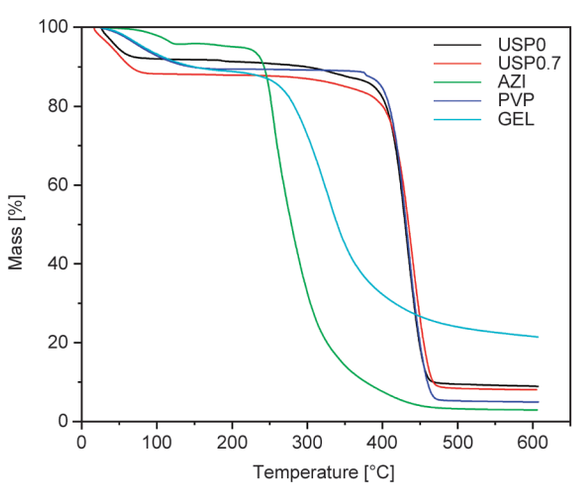

Figure 4. TGA thermograms of AZI, PVP, GEL, and nanofibers.

and all the samples are around 469 °C. The amount of residue left by the samples varies between 0.010 and 0.383 mg. From the thermograms, it was observed that the degradation temperatures of nanofibers were higher than those of AZI and polymers (PVP and GEL). This can be attributed to the weak bond (van der Waals) formation between the polymers and the model drug, as indicated in the FT-IR analysis [49]. Therefore, it shows that the model drug of AZI has been successfully added to the structure of PVP/GEL nanofibers. Finally, it can be said that the thermal stability of the AZI drug substance is increased by nanofiber production since the decomposition temperature of PVP is approximately 158 °C higher than that of AZI, and the decomposition temperature of nanofibers is higher than PVP.

DSC curves of AZI, PVP, GEL, and nanofibers are given in Figure 5.

PVP, which is an amorphous polymer, shows a very wide endotherm due to dehydration, reaching its maximum at 78.9 °C, extending between 29.7 and 137.6 °C [50–52]. This observed peak is expected due to the hygroscopic and amorphous structure of PVP and is due to the water loss of the sample [18]. As the materials become amorphous, the peak indicating the melting point (T_m) may disappear. It is known that the PVP polymer is predominantly amorphous. Also, PVP is a polymer that can be found in a glassy or rubbery form. Therefore, the corresponding Tm peak is quite small [53–57]. As seen in the DSC thermogram of PVP, a small endotherm is seen extending between 174.4 and 190.3 °C, with a peak at 182.5 °C of the T_m point. A very small endothermic transition, known as the softening temperature of the gelatin polymer, was detected at 49.10 °C in the thermogram of pure GEL in powder form [40, 58]. Then, an endotherm peak is observed, starting at 111.58 °C, peaking at 120.30 °C, and ending at 130.28 °C. At this temperature, the triple helix structure of gelatin melts, and randomly distributed structures are formed. The resulting transition enthalpy (ΔH) of 17.68 J/g represents the energy required for the rearrangement of hydrogen bonds, amide bonds, and van der Waals interactions into a random configuration that helps maintain the triple helical structure [59]. This is very common for solid GEL, which always contains some water (normally 10-15%) [60]. In addition, a small endothermic peak at about 213 °C, known as the decomposition temperature of the pure GEL polymer powder, appeared, as is known from the literature [41, 61]. This peak is in agreement with the TGA results. On the DSC thermogram, AZI shows a sharp endothermic peak between 112.92 and 131.52 °C, corresponding to its melting point. This wide endotherm peaked at 125.74 °C [52, 62, 63]. The reason for the wide peak is due to the separation of crystalline water in its structure during melting, as reported in the literature [64]. The melting temperature for this peak was determined to be 88.53 J/g [32]. While different researchers in the literature have reported that AZI samples exhibit variable thermal behavior with a single or two DSC endotherms, the United States Pharmacopeia reference standard has shown it with a single DSC endotherm [48]. In the DSC thermograms of nanofibers, it was clearly seen that the AZI used as a model drug within the scope of the study did not show any melting peak. It has been found that AZI no longer exists as a crystalline material, as is known from the literature; it turns into an amorphous state [45, 65, 66]. While the endotherm peaks of nanofibers coated with thin film with different concentrations of AZI ranged between about 83 and 96 °C, endotherm was detected at around 6 °C in the thermogram of PVP/GEL nanofibers without AZI. From this, it is seen that AZI coating on nanofiber surfaces with the USP technique causes an average of a 20–25 to 25 °C shift in the endotherms of nanofibers.

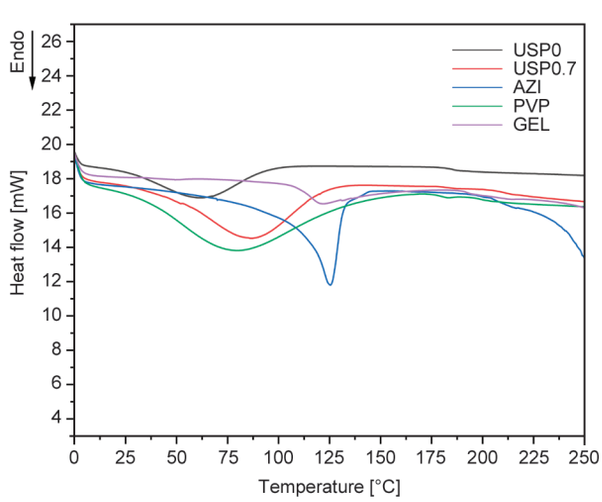

Figure 5. DSC curves of AZI, PVP, GEL, and nanofibers.

XRD diffractograms of AZI, PVP, GEL, and nanofibers are given in Figure 6.

A broad and diffuse mound-shaped peak appeared in the X-ray diffraction of nanofibers. These bump-shaped peaks are due to the amorphous polymers in the structure of nanofibers and appear at around 13° in all diffractograms of nanofibers. The characteristic

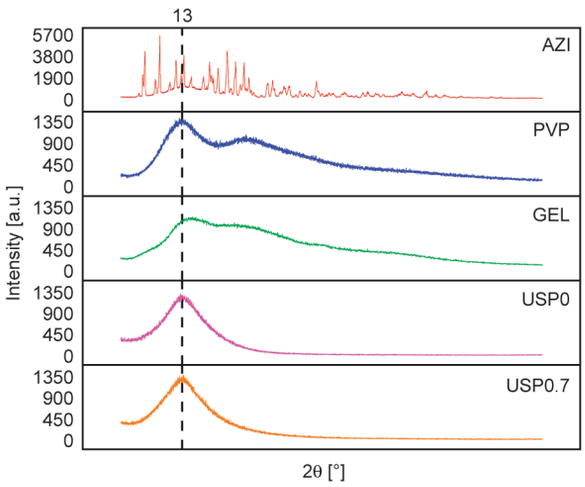

Figure 6. XRD diffractograms of AZI, PVP, GEL, and nanofibers.

peaks of AZI are almost absent in the diffractogram of electrospun nanofibers [47, 67]. This made it clear that AZI is no longer available as a crystalline material but has been completely converted to an amorphous state [50, 68]. DSC and XRD data of nanofibers coated with AZI proved that drug molecules are in an amorphous state in the matrix of PVP/GEL nanofibers. The XRD and DSC result obtained at this stage of the study and the SEM images in which morphological observations were made overlap both with each other and with previous studies involving electrospun nanofibers [51, 69]. Figure 7 shows the cumulative release graphs of nanofiber surfaces coated with different concentrations of AZI by the USP method.

In the USP technique, the model drug AZI is coated on the surface of the nanofibers. Therefore, when the drug-loaded nanofibers were taken into the dissolution medium, they diffused very quickly because they

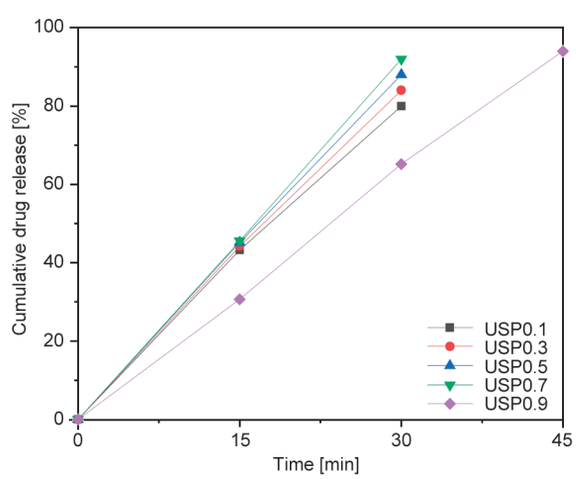

Figure 7. Drug release profiles of different concentrations of AZI-coated nanofibers.

were located on the surface, and the loaded drug was suddenly released as expected. All samples were released with all loaded AZI within the first 30 min. This was attributable to the placement of the drug molecules on the nanofibrous surface. It is clear that drug delivery systems prepared using this method are also suitable for drugs that need burst release.

Here, sandwich structures were formed to prevent the rapid release of the drug from the surface. The main purpose here is to trap the AZI molecules after coating between the nanofibers instead of the surface of the nanofibers. Sandwich structures have been produced to obtain those that can be released more slowly with the USP method. For this, 5 different pure PVP/GEL nanofibers were produced for 1 hour for the bottom layer and coated with USP, containing 0.7% AZI, which was selected optimally in previous release studies. Then, PVP/GEL nanofiber production was carried out for 5, 15, 30, 45, and 60 min for the upper layer. Thanks to the sandwich structures created in this way, the AZI molecules remained between the nanofibers. Then, the release profiles of these sandwich structures were examined, and the effect of the deposition time (5, 15, 30, 45, and 60 min) and nanoweb thickness on the drug release behavior were investigated. In Figure 8, cross-section and surface SEM images of the sandwich structure, which were produced for 60 min on the upper layer (USP 0.7–60), are given.

In Figure 8, it can be clearly seen that the sandwich structure has been successfully achieved. A very small amount of the bead structure seen on the surface was also revealed in the cross-sectional image. In the surface image, it was revealed that the nanofibers are quite thin and smooth. The release profiles of these sandwich structures are given in Figure 9.

When Figure 9 is analyzed, it is seen that as the thickness of the sandwich structures formed increases, the release time also lengthens. Because, in these structures, the drug is located only in the middle layer. There are no drugs on or near the surface of the sandwich structures. Therefore, drug molecules could not diffuse into the dissolution medium quickly. It was determined that the release time increased from 30 min to 2 hours when nanofibers were produced on the drug layer coated with USP for a short time, such as 5 min and up to 2 days when it was produced for 1 hour. While the S0.7 sample, which was loaded with the same amount of drug without forming the sandwich structure, released 80% of the loaded drug

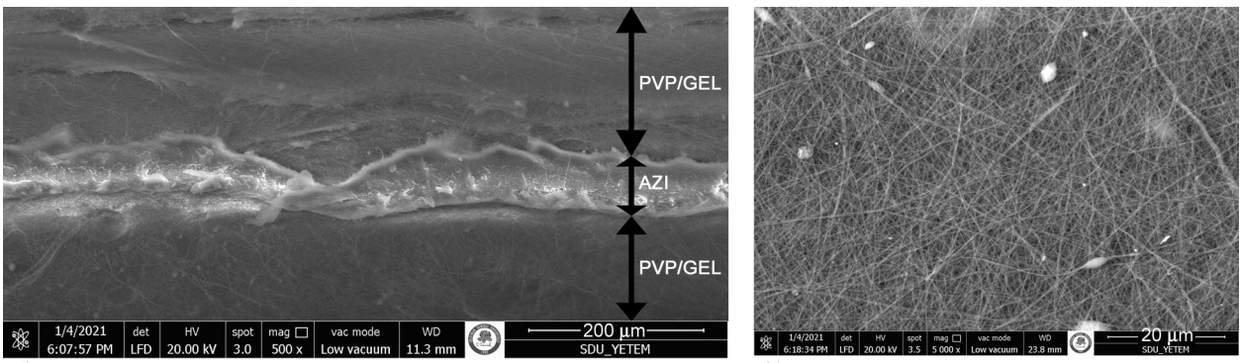

Figure 8. SEM images of sandwich structure a) cross-section image, b) surface image.

in the first 30 min, it released 22.15% when the sandwich was formed for 5 min, and only 9.38% when the sandwich structure was formed for 60 min. Release of the drug in drug delivery systems; the buffer solution is absorbed by the polymer matrix, and after this absorption, the drug diffuses through the polymer matrix. The critical point here is the swelling degree of the polymer matrix. In relation to the increasing surface thickness, the nanofibrous structure has become tighter, the swelling of the surface has slowed down in unit time, and the distance that the drug attached to the nanofibers will travel to diffuse into the dissolution medium has increased [70–72]. These reasons are thought to slow the release rate of the drug.

In the release studies conducted with USP, it has been shown that with this method, drug delivery systems can be used not only in situations where burst release is desired but also long-term release systems can be created by trapping drug molecules in the middle of the sandwich structure. As a result of drug release studies with this method, it has been seen that drug release systems that can produce both burst release and sustained release can be created by using the same method, the same polymer concentrations, and the same amount of drug. Creating systems according to the desired release feature with a single method makes the method advantageous.

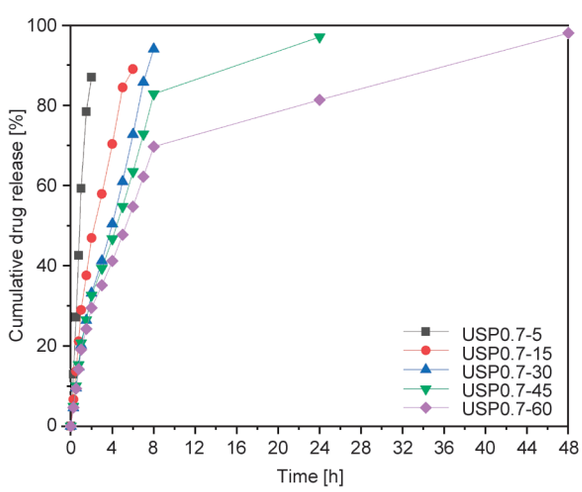

Figure 9. Cumulative drug release profiles of sandwich structures.

4. Conclusions

In this study, PVP/GEL-based nanofiber surfaces were coated with various concentrations of AZI via the USP method. Then, sandwich structures were comprised, and these medical textile surfaces were successfully produced as a drug delivery vehicle. According to the results, nanofibers are quite fine, smooth, and uniform. In the release behaviors of these biomedical materials, after coating with the USP method, the rapid release was observed due to the location of the drug molecules on the nanofibrous surface, and the release occurred in a short time, like 30 min. However, the duration of this period was increased to 48 hours after sandwich constructions were generated at various times. The greatest success of this study was not only in showing that it could use drugs with the USP method but also in the ability of drug delivery systems prepared in this way to have both fast and slow releases.

The results of this study are expected to lay the groundwork for developing new drug delivery systems and other biomedical applications, considering the production method, drug release behaviors, fiber morphology, and the biocompatibility of the raw materials used.

Acknowledgements

This research was supported by Süleyman Demirel University Scientific Research Project Funding Unit, Project No: FDK-2019-6761, and TUBITAK 1002 - Short Term R&D Funding Program, Project No: 119M880. Authors thanks TUBITAK for 2211/C National Ph.D. Scholarship Program in the Priority Fields in Science and Technology and Council of Higher Education 100/2000 Ph.D. Scholarship Program. The authors would like to also thank Assoc. Prof. Dr. Murat KALELİ and Esra ŞEN for their contributions during the USP process.

References

[1] Payab S., Jafari-Aghdam N., Barzegar-Jalali M., Mohammadi G., Lotfipour F., Gholikhani T., Adibkia K.: Preparation and physicochemical characterization of the azithromycin-Eudragit RS100 nanobeads and nanofibers using electrospinning method. Journal of Drug Delivery Science and Technology, **24**, 585–590 (2014). https://doi.org/10.1016/S1773-2247(14)50123-2

[2] Adeli E.: Preparation and evaluation of azithromycin binary solid dispersions using various polyethylene glycols for the improvement of the drug solubility and dissolution rate. Brazilian Journal of Pharmaceutical Sciences, **52**, 1–13 (2016). https://doi.org/10.1590/S1984-82502016000100002

[3] Li X-Y., Li Y-C., Yu D. G., Liao Y-Z., Wang X.: Fast disintegrating quercetin-loaded drug delivery systems fabricated using coaxial electrospinning. International Journal of Molecular Sciences, **14**, 21647–21659 (2013). https://doi.org/10.3390/ijms141121647

[4] Bhowmik D., Harish G., Duraivel S., Kumar B. P., Raghuvanshi V., Kumar K. S.: Solid dispersion-a approach to enhance the dissolution rate of poorly water soluble drugs. The Pharma Innovation, **1**, 24–38 (2013).

[5] Shah J., Vasanti S., Anroop B., Vyas H.: Enhancement of dissolution rate of valdecoxib by solid dispersions technique with PVP K 30 & PEG 4000: Preparation and *in vitro* evaluation. Journal of Inclusion Phenomena and Macrocyclic Chemistry, **63**, 69–75 (2009). https://doi.org/10.1007/s10847-008-9490-9

[6] Patel R. P., Patel M. M.: Physicochemical characterization and dissolution study of solid dispersions of lovastatin with polyethylene glycol 4000 and poly(vinyl pyrrolidone) K30. Pharmaceutical Development and Technology, **12**, 21–33 (2007). https://doi.org/10.1080/10837450601166510

[7] Kesisoglou F., Panmai S., Wu Y.: Nanosizing – Oral formulation development and biopharmaceutical evaluation. Advanced Drug Delivery Reviews, **59**, 631–644 (2007). https://doi.org/10.1016/j.addr.2007.05.003

[8] Szabó E., Démuth B., Nagy B., Molnár K., Farkas A., Szabó B., Balogh A., Hirsch E., Nagy B., Marosi Gy., Nagy Z. K.: Scaled-up preparation of drug-loaded electrospun polymer fibres and investigation of their continuous processing to tablet form. Express Polymer Letters, **12**, 436–451 (2018). https://doi.org/10.3144/expresspolymlett.2018.37

[9] del Valle L. J., Díaz A., Royo M., Rodríguez-Galán A., Puiggalí J.: Biodegradable polyesters reinforced with triclosan loaded polylactide micro/nanofibers: Properties, release and biocompatibility. Express Polymer Letters, **6**, 266–282 (2012). https://doi.org/10.3144/expresspolymlett.2012.30

[10] Amalorpava Mary L., Senthilram T., Suganya S., Nagarajan L., Venugopal J., Ramakrishna S., Giri Dev V.: Centrifugal spun ultrafine fibrous web as a potential drug delivery vehicle. Express Polymer Letters, **7**, 238–248 (2013). https://doi.org/10.3144/expresspolymlett.2013.22

[11] Nagy Zs. K., Nyúl K., Wagner I., Molnár K., Marosi Gy.: Electrospun water soluble polymer mat for ultrafast release of Donepezil HCL. Express Polymer Letters, **4**, 763–772 (2010). https://doi.org/10.3144/expresspolymlett.2010.92

[12] Gao S., Liu Y., Jiang J., Li X., Ye F., Fu Y., Zhao L.: Thiram/hydroxypropyl-β-cyclodextrin inclusion complex electrospun nanofibers for a fast dissolving water-based drug delivery system. Colloids and Surfaces B: Biointerfaces, **201**, 111625 (2021). https://doi.org/10.1016/j.colsurfb.2021.111625

[13] Almeida C., Lovisa L., Santiago A., Li M., Longo E., Paskocimas C., Motta F., Bomio M.: One-step synthesis of $CaMoO_4$: Eu^{3+} nanospheres by ultrasonic spray pyrolysis. Journal of Materials Science: Materials in Electronics, **28**, 16867–16879 (2017). https://doi.org/10.1007/s10854-017-7605-z

[14] Das H., Debnath N., Toda A., Kawaguchi T., Sakamoto N., Aono H., Shinozaki K., Suzuki H., Wakiya N.: Impact of precursor solution concentration to form superparamagnetic $MgFe_2O_4$ nanospheres by ultrasonic spray pyrolysis technique for magnetic thermotherapy. Advanced Powder Technology, **28**, 1696–1703 (2017). https://doi.org/10.1016/j.apt.2017.04.007

[15] Kundu M., Karunakaran G., Kolesnikov E., Sergeevna V. E., Kumari S., Gorshenkov M. V., Kuznetsov D.: Hollow $NiCo_2O_4$ nano-spheres obtained by ultrasonic spray pyrolysis method with superior electrochemical performance for lithium-ion batteries and supercapacitors. Journal of Industrial and Engineering Chemistry, **59**, 90–98 (2018). https://doi.org/10.1016/j.jiec.2017.10.010

[16] Lv L., Cheng P., Wang Y., Xu L., Zhang B., Lv C., Ma J., Zhang Y.: Sb-doped three-dimensional $ZnFe_2O_4$ macroporous spheres for *N*-butanol chemiresistive gas sensors. Sensors and Actuators B: Chemical, **320**, 128384 (2020). https://doi.org/10.1016/j.snb.2020.128384

[17] Skrabalak S. E., Suslick K. S.: Porous MoS_2 synthesized by ultrasonic spray pyrolysis. Journal of the American Chemical Society, **127**, 9990–9991 (2005). https://doi.org/10.1021/ja051654g

[18] Adeli E.: Irbesartan-loaded electrospun nanofibers-based PVP K90 for the drug dissolution improvement: Fabrication, *in vitro* performance assessment, and *in vivo* evaluation. Journal of Applied Polymer Science, **132**, 42212 (2015). https://doi.org/10.1002/app.42212

[19] Zhang Y., Liu X., Cui Y., Huang H., Chi N., Tang X.: Aspects of degradation kinetics of azithromycin in aqueous solution. Chromatographia, **70**, 67–73 (2009). https://doi.org/10.1365/s10337-009-1116-x

[20] Taghe S., Mehrandish S., Mirzaeei S.: Preparation of azithromycin nanofibers as controlled release ophthalmic drug carriers using electrospinning technique: *In vitro* and *in vivo* characterization. Advanced Pharmaceutical Bulletin, **12**, 346–355 (2022). https://doi.org/10.34172/apb.2022.033

[21] Alimohammadi M., Fakhraei O., Moradi A., Kabiri M., Moradi A., Passandideh-Fard M., Tamayol A., Ebrahimzadeh M. H., Shaegh S. A. M.: Controlled release of azithromycin from polycaprolactone/chitosan nanofibrous membranes. Journal of Drug Delivery Science and Technology, **71**, 103246 (2022). https://doi.org/10.1016/j.jddst.2022.103246

[22] Bang J. H., Han K., Skrabalak S. E., Kim H., Suslick K. S.: Porous carbon supports prepared by ultrasonic spray pyrolysis for direct methanol fuel cell electrodes. The Journal of Physical Chemistry C, **111**, 10959–10964 (2007). https://doi.org/10.1021/jp071624v

[23] Krasnikova I. V., Mishakov I. V., Bauman Y. I., Karnaukhov T. M., Vedyagin A. A.: Preparation of NiO-CuO-MgO fine powders by ultrasonic spray pyrolysis for carbon nanofibers synthesis. Chemical Physics Letters, **684**, 36–38 (2017). https://doi.org/10.1016/j.cplett.2017.06.036

[24] Zhang J., Khatri I., Kishi N., Mominuzzaman S. M., Soga T., Jimbo T.: Low substrate temperature synthesis of carbon nanowalls by ultrasonic spray pyrolysis. Thin Solid Films, **519**, 4162–4165 (2011). https://doi.org/10.1016/j.tsf.2011.02.006

[25] Zhang X., Luo X., Han J., Li J., Han W.: Electronic structure, elasticity and hardness of diborides of zirconium and hafnium: First principles calculations. Computational Materials Science, **44**, 411–421 (2008). https://doi.org/10.1016/j.commatsci.2008.04.002

[26] Suh W. H., Suslick K. S.: Magnetic and porous nanospheres from ultrasonic spray pyrolysis. Journal of the American Chemical Society, **127**, 12007–12010 (2005). https://doi.org/10.1021/ja050693p

[27] Kawanobe Y., Honda M., Konishi T., Mizumoto M., Habuto Y., Kanzawa N., Uchino T., Aizawa M.: Preparation of apatite microsphere with nano-size pores on the surface *via* salt-assisted ultrasonic spray-pyrolysis technique and its drug release behavior. Journal of the Australian Ceramics Society, **46**, 6–10 (2010).

[28] Matsueda M., Yoshihisa H., Emoto M., Aizawa M.: 1Pb-59 synthesis of calcium-phosphate microsphere by ultrasonic spray-pyrolysis technique and its application to drug delivery system. in 'Proceedings of Symposium on Ultrasonic Electronics, Város, Ország' Vol. **31**, 259–260 (2010). https://doi.org/10.24492/use.31.0_259

[29] Sambudi N. S., Cho S., Cho K.: Porous hollow hydroxyapatite microspheres synthesized by spray pyrolysis using a microalga template: Preparation, drug delivery, and bioactivity. RSC Advances, **6**, 43041–43048 (2016). https://doi.org/10.1039/C6RA03147A

[30] Ardekani S. R., Aghdam A. S. R., Nazari M., Bayat A., Yazdani E., Saievar-Iranizad E.: A comprehensive review on ultrasonic spray pyrolysis technique: Mechanism, main parameters and applications in condensed matter. Journal of Analytical and Applied Pyrolysis, **141**, 104631 (2019). https://doi.org/10.1016/j.jaap.2019.104631

[31] Cengiz F., Jirsak O.: The effect of salt on the roller electrospinning of polyurethane nanofibers. Fibers and Polymers, **10**, 177–184 (2009). https://doi.org/10.1007/s12221-009-0177-7

[32] Bakheit A. H., Al-Hadiya B. M., Abd-Elgalil A. A.: Azithromycin. in 'Profiles of drug substances, excipients and related methodology' (ed.: Brittain H. G.) Elsevier, Vol. 39, 1–40 (2014). https://doi.org/10.1016/B978-0-12-800173-8.00001-5

[33] Güler H. K., Çallıoğlu F. C.: Two-step crosslinking of PVP/GEL nanofibers. in 'The 10th International Conferance TEXTEH 2021. Bucharest, Romania', Vol. 164–170 (2021). https://doi.org/10.35530/TT.2021.25

[34] Borodko Y., Habas S. E., Koebel M., Yang P., Frei H., Somorjai G. A.: Probing the interaction of poly(vinyl pyrrolidone) with platinum nanocrystals by UV-Raman and FTIR. The Journal of Physical Chemistry B, **110**, 23052–23059 (2006). https://doi.org/10.1021/jp063338+

[35] Kim G-M., Le K. H. T., Giannitelli S. M., Lee Y. J., Rainer A., Trombetta M.: Electrospinning of PCL/PVP blends for tissue engineering scaffolds. Journal of Materials Science: Materials in Medicine, **24**, 1425–1442 (2013). https://doi.org/10.1007/s10856-013-4893-6

[36] Laot C. M., Marand E., Oyama H. T.: Spectroscopic characterization of molecular interdiffusion at a poly (vinyl pyrrolidone)/vinyl ester interface. Polymer, **40**, 1095–1108 (1999). https://doi.org/10.1016/S0032-3861(98)80003-7

[37] Reksamunandar R. P., Edikresnha D., Munir M. M., Damayanti S., Khairurrijal: Encapsulation of β-carotene in poly(vinyl pyrrolidone)(PVP) by electrospinning technique. Procedia Engineering, **170**, 19–23 (2017). https://doi.org/10.1016/j.proeng.2017.03.004

[38] Torres-Giner S., Wilkanowicz S., Melendez-Rodriguez B., Lagaron J. M.: Nanoencapsulation of aloe vera in synthetic and naturally occurring polymers by electrohydrodynamic processing of interest in food technology and bioactive packaging. Journal of Agricultural and Food Chemistry, **65**, 4439–4448 (2017). https://doi.org/10.1021/acs.jafc.7b01393

[39] Yu D-G., Shen X-X., Branford-White C., White K., Zhu L-M., Bligh S. A.: Oral fast-dissolving drug delivery membranes prepared from electrospun poly(vinyl pyrrolidone) ultrafine fibers. Nanotechnology, **20**, 055104 (2009). https://doi.org/10.1088/0957-4484/20/5/055104

[40] Dhandayuthapani B., Krishnan U. M., Sethuraman S.: Fabrication and characterization of chitosan-gelatin blend nanofibers for skin tissue engineering. Journal of Biomedical Materials Research Part B: Applied Biomaterials, **94**, 264–272 (2010). https://doi.org/10.1002/jbm.b.31651

[41] Ki C. S., Baek D. H., Gang K. D., Lee K. H., Um I. C., Park Y. H.: Characterization of gelatin nanofiber prepared from gelatin–formic acid solution. Polymer, **46**, 5094–5102 (2005). https://doi.org/10.1016/j.polymer.2005.04.040

[42] Kim M. S., Jun I., Shin Y. M., Jang W., Kim S. I., Shin H.: The development of genipin-crosslinked poly(caprolactone) (PCL)/gelatin nanofibers for tissue engineering applications. Macromolecular Bioscience, **10**, 91–100 (2010). https://doi.org/10.1002/mabi.200900168

[43] Ko J. H., Yin H., An J., Chung D. J., Kim J. H., Lee S. B., Pyun D. G.: Characterization of cross-linked gelatin nanofibers through electrospinning. Macromolecular Research, **18**, 137–143 (2010). https://doi.org/10.1007/s13233-009-0103-2

[44] Nguyen T-H., Lee B-T.: Fabrication and characterization of cross-linked gelatin electro-spun nano-fibers. Journal of Biomedical Science and Engineering, **3**, 1117–1124 (2010). https://doi.org/10.4236/jbise.2010.312145

[45] Ghari T., Mortazavi S., Khoshayand M., Kobarfard F., Gilani K.: Preparation, optimization, and *in vitro* evaluation of azithromycin encapsulated nanoparticles by using response surface methodology. Journal of Drug Delivery Science and Technology, **24**, 352–360 (2014). https://doi.org/10.1016/S1773-2247(14)50073-1

[46] Khalil I. A., Ali I. H., El-Sherbiny I. M.: Noninvasive biodegradable nanoparticles-in-nanofibers single-dose ocular insert: *In vitro*, *ex vivo* and *in vivo* evaluation. Nanomedicine, **14**, 33–55 (2019). https://doi.org/10.2217/nnm-2018-0297

[47] Mohammadi G., Valizadeh H., Barzegar-Jalali M., Lotfipour F., Adibkia K., Milani M., Azhdarzadeh M., Kiafar F., Nokhodchi A.: Development of azithromycin–PLGA nanoparticles: Physicochemical characterization and antibacterial effect against *Salmonella typhi*. Colloids and Surfaces B: Biointerfaces, **80**, 34–39 (2010). https://doi.org/10.1016/j.colsurfb.2010.05.027

[48] Timoumi S., Mangin D., Peczalski R., Zagrouba F., Andrieu J.: Stability and thermophysical properties of azithromycin dihydrate. Arabian Journal of Chemistry, **7**, 189–195 (2014). https://doi.org/10.1016/j.arabjc.2010.10.024

[49] Li D., Nie W., Chen L., Miao Y., Zhang X., Chen F., Yu B., Ao R., Yu B., He C.: Fabrication of curcumin-loaded mesoporous silica incorporated polyvinyl pyrrolidone nanofibers for rapid hemostasis and antibacterial treatment. RSC Advances, **7**, 7973–7982 (2017). https://doi.org/10.1039/C6RA27319J

[50] Dai X-Y., Nie W., Wang Y-C., Shen Y., Li Y., Gan S-J.: Electrospun emodin polyvinylpyrrolidone blended nanofibrous membrane: A novel medicated biomaterial for drug delivery and accelerated wound healing. Journal of Materials Science: Materials in Medicine, **23**, 2709–2716 (2012). https://doi.org/10.1007/s10856-012-4728-x

[51] Illangakoon U. E., Nazir T., Williams G. R., Chatterton N. P.: Mebeverine-loaded electrospun nanofibers: Physicochemical characterization and dissolution studies. Journal of Pharmaceutical Sciences, **103**, 283–292 (2014). https://doi.org/10.1002/jps.23759

[52] Li X-Y., Wang X., Yu D-G., Ye S., Kuang Q-K., Yi Q-W., Yao X-Z.: Electrospun borneol-PVP nanocomposites. Journal of Nanomaterials, **2012**, 731382 (2012). https://doi.org/10.1155/2012/731382

[53] Jadhav N. R., Gaikwad V. L., Nair K. J., Kadam H. M.: Glass transition temperature: Basics and application in pharmaceutical sector. Asian Journal of Pharmaceutics, **3**, 82–89 (2009). https://doi.org/10.4103/0973-8398.55043

[54] Qian W., Yu D-G., Li Y., Li X-Y., Liao Y-Z., Wang X.: Triple-component drug-loaded nanocomposites prepared using a modified coaxial electrospinning. Journal of Nanomaterials, **2013**, 826471 (2013). https://doi.org/10.1155/2013/826471

[55] Saroj A., Singh R., Chandra S.: Studies on polymer electrolyte poly(vinyl pyrrolidone) (PVP) complexed with ionic liquid: Effect of complexation on thermal stability, conductivity and relaxation behaviour. Materials Science and Engineering: B, **178**, 231–238 (2013). https://doi.org/10.1016/j.mseb.2012.11.007

[56] Yu D. G., Wang X., Li X. Y., Chian W., Li Y., Liao Y. Z.: Electrospun biphasic drug release poly(vinyl pyrrolidone)/ethyl cellulose core/sheath nanofibers. Acta Biomaterialia, **9**, 5665–5672 (2013). https://doi.org/10.1016/j.actbio.2012.10.021

[57] Yu D-G., Gao L-D., White K., Branford-White C., Lu W-Y., Zhu L-M.: Multicomponent amorphous nanofibers electrospun from hot aqueous solutions of a poorly soluble drug. Pharmaceutical Research, **27**, 2466–2477 (2010).
https://doi.org/10.1007/s11095-010-0239-y

[58] Chen H-C., Jao W-C., Yang M-C.: Characterization of gelatin nanofibers electrospun using ethanol/formic acid/water as a solvent. Polymers for Advanced Technologies, **20**, 98–103 (2009).
https://doi.org/10.1002/pat.1244

[59] Jalaja K., James N. R.: Electrospun gelatin nanofibers: A facile cross-linking approach using oxidized sucrose. International Journal of Biological Macromolecules, **73**, 270–278 (2015).
https://doi.org/10.1016/j.ijbiomac.2014.11.018

[60] Zhang Y. Z., Venugopal J., Huang Z-M., Lim C. T., Ramakrishna S.: Crosslinking of the electrospun gelatin nanofibers. Polymer, **47**, 2911–2917 (2006).
https://doi.org/10.1016/j.polymer.2006.02.046

[61] Song J-H., Kim H-E., Kim H-W.: Production of electrospun gelatin nanofiber by water-based *co*-solvent approach. Journal of Materials Science: Materials in Medicine, **19**, 95–102 (2008).
https://doi.org/10.1007/s10856-007-3169-4

[62] Aucamp M., Odendaal R., Liebenberg W., Hamman J.: Amorphous azithromycin with improved aqueous solubility and intestinal membrane permeability. Drug Development and Industrial Pharmacy, **41**, 1100–1108 (2015).
https://doi.org/10.3109/03639045.2014.931967

[63] Tung N-T., Tran C-S., Nguyen T-L., Hoang T., Trinh T-D., Nguyen T-N.: Formulation and biopharmaceutical evaluation of bitter taste masking microparticles containing azithromycin loaded in dispersible tablets. European Journal of Pharmaceutics and Biopharmaceutics, **126**, 187–200 (2018).
https://doi.org/10.1016/j.ejpb.2017.03.017

[64] Kauss T., Gaubert A., Boyer C., Ba B. B., Manse M., Massip S., Léger J-M., Fawaz F., Lembege M., Boiron J-M., LafargeX., Lindegardh N., With N. J., Olliaro P., Millet P., Gaudin K.: Pharmaceutical development and optimization of azithromycin suppository for paediatric use. International Journal of Pharmaceutics, **441**, 218–226 (2013).
https://doi.org/10.1016/j.ijpharm.2012.11.040

[65] Gandhi R., Pillai O., Thilagavathi R., Gopalakrishnan B., Kaul C. L., Panchagnula R.: Characterization of azithromycin hydrates. European Journal of Pharmaceutical Sciences, **16**, 175–184 (2002).
https://doi.org/10.1016/s0928-0987(02)00087-8

[66] Tonglairoum P., Ngawhirunpat T., Rojanarata T., Kaomongkolgit R., Opanasopit P.: Fast-acting clotrimazole composited PVP/HPβCD nanofibers for oral candidiasis application. Pharmaceutical Research, **31**, 1893–1906 (2014).
https://doi.org/10.1007/s11095-013-1291-1

[67] Jasanada M. S. B., Garcia I. L., Mari F. F.: Azithromycin preparation in its noncryst alline and crystalline dihydrate forms. U.S. Patent 6451990B1, USA (2002).

[68] Huang L-Y., Branford-White C., Shen X-X., Yu D-G., Zhu L-M.: Time-engineeringed biphasic drug release by electrospun nanofiber meshes. International Journal of Pharmaceutics, **436**, 88–96 (2012).
https://doi.org/10.1016/j.ijpharm.2012.06.058

[69] Verreck G., Chun I., Peeters J., Rosenblatt J., Brewster M. E.: Preparation and characterization of nanofibers containing amorphous drug dispersions generated by electrostatic spinning. Pharmaceutical research, **20**, 810–817 (2003).
https://doi.org/10.1023/A:1023450006281

[70] Akduman Ç.: Development of electrospun textile materials for drug relase. Ph. D. Thesis, 268p, Ege University, Izmir, Turkey (2015).

[71] Hamidi M., Azadi A., Rafiei P.: Hydrogel nanoparticles in drug delivery. Advanced Drug Delivery Reviews, **60**, 1638–1649 (2008).
https://doi.org/10.1016/j.addr.2008.08.002

[72] Taepaiboon P., Rungsardthong U., Supaphol P.: Drug-loaded electrospun mats of poly(vinyl alcohol) fibres and their release characteristics of four model drugs. Nanotechnology, **17**, 2317 (2006).
https://doi.org/10.1088/0957-4484/17/9/041